Journal of the European Ceramic Society 16 (1996) 413–420

0955-2219(95)00129-8
0955-2219/96/$15.00

Liquid Phase Sintering of Silicon Carbide

F. K. van Dijen & E. Mayer

Jestettenerstrasse 6, 79802 Baltersweil, Germany

(Received 13 August 1993; revised version received 3 July 1995; accepted 14 July 1995)

Abstract

It is shown that the decomposition reactions during the sintering of liquid phase silicon carbide (SiC) can be described well by thermodynamics. This allows for an optimization of the sintering parameters. The use of carbon as a sintering additive, together with, for instance, yttria plus alumina, is of advantage. When C is used, SiO_2 will not occur in the liquid phase during sintering or in the amorphous and crystalline phases after sintering. The microstructure of sintered samples is described.

1 Introduction

Liquid phase sintered silicon carbide (LP-SiC) has the potential to become an alternative, commercially attractive, sintered SiC material, because it can be ('pressureless') sintered without a powder bed and because relatively cheap raw materials and sintering additives can be used. The literature on LP-SiC is scattered, with the main topics of interest being the sintering process, the microstructure of the sintered material and the resulting properties.[1–16] References for the individual topics are indicated in the following paragraphs.

The most important factors which control the liquid phase sintering of SiC are: the specific surface area of the SiC powder, the sintering atmosphere (N_2 or Ar), the amount and composition of the liquid phase, the use of a powder bed, the sintering time, the sintering temperature and, of course, the processing methods used prior to firing. The usual sintering additives are alumina + yttria with an alumina:yttria weight ratio >1.[1] Typically 5–15 wt% of the sintering additives are used. The higher the amount of sintering additives, the higher the sintering rate.[2] Other sintering additives instead of yttria + alumina are: magnesia + alumina,[3] other rare earth metal oxides + alumina,[4] alumina,[5] sialon[6] or yttria + aluminium nitride.[7]

We carried out a literature survey, as well as experiments to verify the results presented in the literature, resulting in an assessment of the state-of-the-art for LP-SiC, as presented below.

The sintering temperature in Ar is ~1900°C.[3,4,8,9] The sintering temperature in N_2 is ~2100°C.[1,4] We found a sintering time of ~2 h. A few per cent weight loss of the sample is always observed. We observed a higher weight loss upon sintering in N_2 than in Ar. We also observed more grain growth upon sintering in N_2 than in Ar. These phenomena can be explained by the higher sintering temperature required in N_2, compared to Ar. The use of closed containers and a powder bed reduces the weight losses.[9,10] We observed that the material sintered in N_2 picks up ~1 wt% N and that weight loss is related to a reduction of the oxygen content of the material. A SiC powder with a specific surface area of >5 m^2 g^{-1} has to be used; for instance a SiC powder with a specific surface area of 10 or 15 m^2 g^{-1}.[11] We found that the higher the specific surface area of the SiC powder, the higher the sintering rate. It was shown that good mixing of the SiC powder with the sintering additives is necessary. We discovered that CeO_2 is a cheaper but less effective sintering additive, compared to yttria. La_2O_3 proved to be a cheaper and effective sintering additive. By using La_2O_3 instead of yttria, one has to increase the sintering temperature in Ar by ~50°C.

The microstructure of LP-SiC is characterized by the absence of exaggerated grain growth and by a small average grain size.[7,11,12] By annealing the sintered material, the grain boundary phase can be completely removed from the grain boundaries and crystallized at the triple points.[8,11,12] By good processing, the presence of large pores can be prevented. Sintered densities of more than 3·15 g ml^{-1} are obtained.

Compared to SiC sintered with B and C, LP-SiC has a strength which is twice as high.[5,7,8,12] This high strength is related to the much higher fracture toughness and to a change from transcrystalline to intercrystalline fracture behaviour.[5,8,10,12] We obtained a material with a K_{ic} value of 6–7 MPa $m^{1/2}$, as determined by the indentation technique. The microhardness is ~26 GPa, which is

similar to that of SiC sintered with B and C. Little has been published on the properties of LP-SiC and the relations between the different microstructures and the properties.

The goal of the present work is to optimize the processing and sintering of LP-SiC. The microstructures of the sintered materials that have been obtained are shown and discussed.

2 Theoretical Aspects

The liquid phase sintering of SiC in Ar is influenced by the phase relations between SiC and the sintering additives, for instance yttria + alumina, by the extent of wetting of the SiC by the liquid phase and by the solubility of SiC in the liquid phase. As will be shown, SiO_2 present as surface silica on the SiC powder plays a very different role in the sintering process compared to the surface silica on Si_3N_4 powder. There is competition between the sintering and decomposition reactions which result in weight losses. The most important decomposition reactions are:

$$2SiO_2 + SiC = 3SiO + CO \quad (1)$$

$$Al_2O_3 + SiC = SiO + Al_2O + CO \quad (2)$$

Reaction (1) can be prevented by adding carbon, as in the sintering of SiC with B and C. By adding carbon the following reaction will occur:

$$SiO_2 + 3C = SiC + 2CO \quad (3)$$

To remove the 1 wt% oxygen present as surface silica on the SiC particles, one has to add 1·13 wt% carbon relative to the SiC powder. SiC powder typically contains ~0·1 wt% oxygen $(m^2\ g^{-1})^{-1}$.[13] The changes in Gibbs free energy for reactions (1)–(3) are:

$$G°_T = 384\,400 - 165{\cdot}4\ T\ (J) \quad (4)$$

$$G°_T = 1\,369\,700 - 551{\cdot}6\ T\ (J) \quad (5)$$

$$G°_T = 604\,000 - 339{\cdot}4\ T\ (J) \quad (6)$$

The total gas pressure resulting from reactions (1)–(3) can be calculated from eqns (4)–(6). The results of these calculations are given in Table 1.

Table 1. Total gas pressure (in bar) as a function of temperature, according to reactions (l)–(3)

Temperature (°C)	*Reaction*					
	1	*2*	*3*	*1**	*2**	*3**
1600	0·53	0·002	2·8	0·17	0·002	0·87
1800	0·96	0·038	18	0·30	0·030	5·7
2000	1·6	0·39	84	0·50	0·30	27
2200	2·4	2·7	306	0·75	2·2	97

*The activity of alumina is taken as 0·5 and the activity of silica is taken as 0·1.

For these calculations, the activity of the solids (SiC, SiO_2, Al_2O_3 and C) is taken as 1. One set of calculations is made with an activity for alumina of 0·5 and an activity for silica of 0·1, to allow for the case where an alumina–yttria–silica compound is the reactant instead of pure alumina or silica.

From Table 1 it can be seen that, from a thermodynamic point of view, reaction (3) is favoured over reaction (1). Reaction (2) becomes very important at temperatures higher than about 2000°C, which is the sintering condition in N_2. Reaction (2) will play a less significant role when the material is sintered in Ar, a process which is carried out at 1900°C. The addition of carbon should result in a significantly lower weight loss when the material is sintered in Ar because SiO should not be formed. The addition of carbon is also an advantage from the processing point of view, as it acts as a lubricant in shaping methods such as dry pressing and extrusion. From Table 1 it also becomes clear that some weight loss cannot be prevented, since reactions (1) and (3) will always occur (the total gas pressure is higher than 1 bar under the sintering conditions). This also shows that most, if not all, of the originally present silica will be lost from the sintered material. Reactions (1) and (3) must be allowed to finish before the pores close, otherwise large pores and even cracks may form in the sintered material.

The rare earth metal oxides seem stable, from a thermodynamic point of view, under the sintering conditions. However, magnesia seems less stable. When the material is sintered in N_2 the following reaction may occur:

$$3SiC + 2Al_2O_3 + N_2 = 4AlN + 3SiO + 3CO \quad (7)$$

Sintering in Ar is consequently favoured over sintering in N_2; the proper amount of carbon should also be used as a sintering additive.

The crucial aspect of the microstructure of LP-SiC, besides the absence of exaggerated grain growth, seems to be the presence or absence of a grain boundary phase. Such a phase would be expected to influence the oxidation resistance, the high-temperature strength, the creep resistance and the electrical conductivity of LP-SiC.[14] As mentioned before, this grain boundary phase can be removed by an annealing process after sintering.[8,11] Due to the absence of silica, crystalline phases are expected to form at the triple points, because silica is well known as the main vitrifying component.

3 Experimental Procedures

As SiC powder, UFB-10 from Lonza-Werke, Waldshut, Germany was used. This powder has a

specific surface area of 10 $m^2 g^{-1}$ and contains ~1·0 wt% oxygen and 0·2 wt% aluminium. The yttria powder was from Sassoon, Brussels, Belgium, the alumina powder, type CS 400, from Martinswerk, Bergheim, Germany and the carbon black, type FW-18, from Degussa, Hanau, Germany. The SiC powder was mixed with the sintering additives in demineralized water using a polyurethane-lined grinder and sintered SiC media with a diameter of 3 mm. Dispersing agents (Triton X-100, Union Carbide, 3 wt% and triethanolamine, Merck, 2 wt%), an antifoam agent (SE-34, Wacker Chemie, 0·5 wt%) and a lubricant (polyethyleneglycol-400, Hoechst, 3 wt%) were also added. The percentages are relative to the SiC plus sintering additives. After mixing, the suspension was dried at 100°C overnight. The dried cake was broken in a mortar and screened over a 0·3 mm screen. The granulate was uniaxially pressed at 100 MPa and organic additives were removed by heating the tablets at 300°C for 8 h in air. The green density of the tablets after removal of the organic additives was 1·70 g ml^{-1}.

Next, the tablets were sintered in a closed graphite crucible, using the powder bed technique. The powder bed consisted of 61 wt% SiC UFB-10, 32 wt% BN, 3 wt% yttria and 4 wt% alumina. The other experimental conditions are listed in Table 2. After sintering the density and the weight loss of the sintered tablets were measured. The sintered tablets were cut, ground and polished using diamond tools. The Vickers microhardness was determined using a 100 g load. The polished samples were plasma-etched and the microstructure was studied using SEM at the Max Planck Institut für Metallforschung, Stuttgart, Germany. This technique reveals the grain size distribution in the sintered material. The sintered samples were cut, thinned and investigated using TEM with EDX at the University of Technology, Zürich, Switzerland. This method shows, amongst other aspects, the presence of a grain boundary phase. Samples were observed after sintering with XRD to reveal the crystalline phases present.

Table 2. Most important experimental parameters

Experiment	*Composition (wt%)*			*Sintering time (h)*		
	Y_2O_3	Al_2O_3	C		*Temperature (°C)*	*Atmosphere*
1	4	6	1	2	1900	Ar
2	4	6	—	2	1900	Ar
3	4	6	1	2	2100	N_2
4	4	6	—	2	2100	N_2

4 Results

The results of the experiments are summarized in Table 3. They indicate that the density and microhardness are similar for all experiments. The tablets sintered in N_2 at 2100°C show a higher weight loss than the tablets sintered in Ar at 1900°C. The sample sintered in Ar with C as a sintering additive shows less weight loss than the sample sintered in Ar without C. The materials sintered in N_2 at 2100°C have larger grains than the material sintered in Ar at 1900°C.

Figures 1–4 show scanning electron micrographs of the sintered materials. A quantitative microstructural analysis revealed clear differences in average grain size between the samples (Table 3).

Fig. 1. Electron micrograph of sample 1, for material sintered with C in Ar at 1900°C. The length of the bar is 2 μm.

Table 3. Results of experiments

Experiment	*Weight loss (wt%)*	*Density (g ml^{-1})*	*Hardness (GPa)*	*Grain size (μm)*	*Average grain size (μm)*	*Second-phase material*
1	2·5	3·20	26·4	<4	2·0	YAG Y–Al–O–C
2	3·5	3·18	26·4	<4	1·9	YAG Y–Al–Si–O
3	7·0	3·21	26·4	<6	3·4	Y_2O_3, YAG AlN
4	7·5	3·18	26·0	<4	3·0	Y_2O_3, YAG AlN

Fig. 2. Electron micrograph of sample 2, for material sintered without C in Ar at 1900°C. The length of the bar is 2 μm.

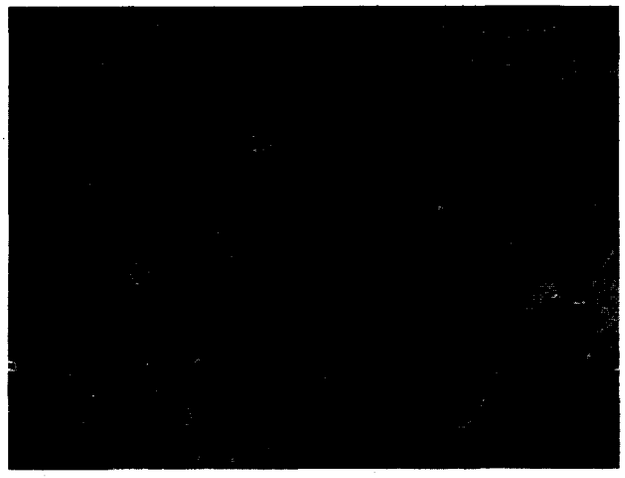

Fig. 3 Electron micrograph of sample 3, for material sintered with C in N_2 at 2100°C. The length of the bar is 2 μm.

Fig. 4. Electron micrograph of sample 4, for material sintered without C in N_2 at 2100°C. The length of the bar is 2 μm.

Figures 5–14 show transmission electron micrographs of the sintered materials. Figure 5 shows the rounded grains in sample 1. Figure 6 shows a triple point in sample 1. Note the poor wetting of the SiC grains by the second phase, as indicated by an angle between 50 and 80°.[14] The second

Fig. 5. Transmission electron micrograph of sample 1, for material sintered with C in Ar at 1900°C, showing rounded grains. The length of the bar is 3·1 μm.

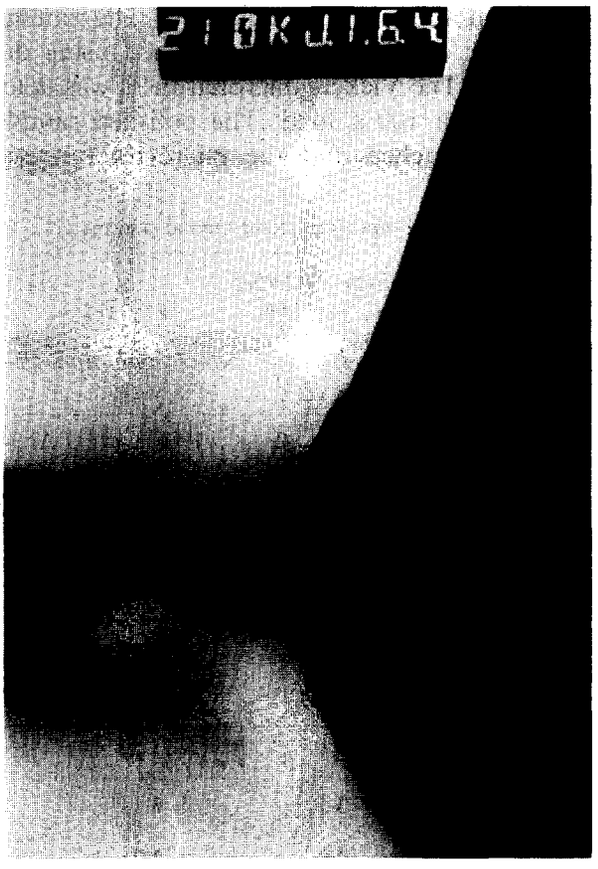

Fig. 6. Transmission electron micrograph of sample 1, for material sintered with C in Ar at 1900°C, showing a triple point. The length of the bar is 120 nm.

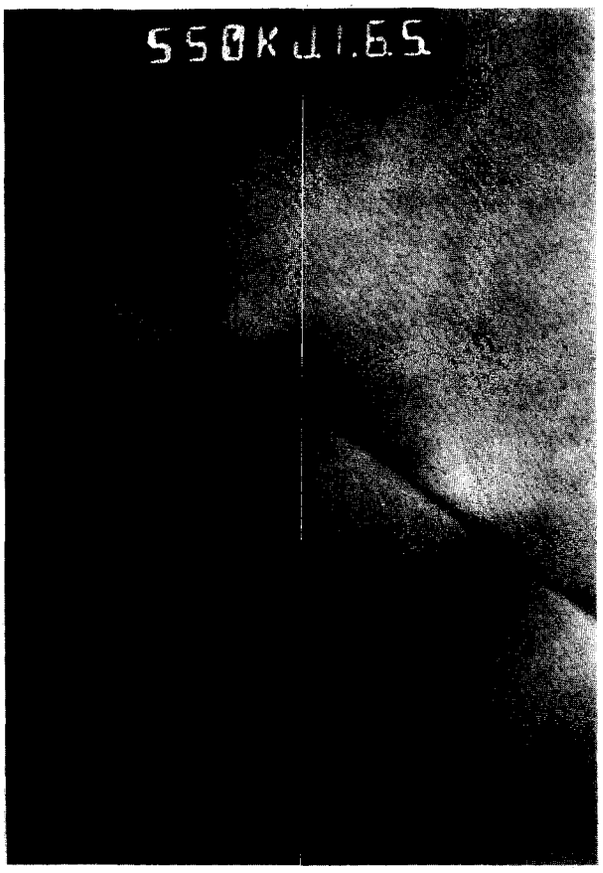

Fig. 7. Transmission electron micrograph of sample 1, for material sintered with C in Ar at 1900°C, showing the grain boundary phase. The length of the bar is 46 nm.

Fig. 9. Transmission electron micrograph of sample 2, for material sintered without C in Ar at 1900°C, showing a triple point. The length of the bar is 120 nm.

Fig. 8. Transmission electron micrograph of sample 2, for material sintered without C in Ar at 1900°C, showing rounded grains. The length of the bar is 3·1 μm.

Fig. 10. Transmission electron micrograph of sample 3, for material sintered with C in N_2 at 2100°C, showing SiC grains. The length of the bar is 3·1 μm.

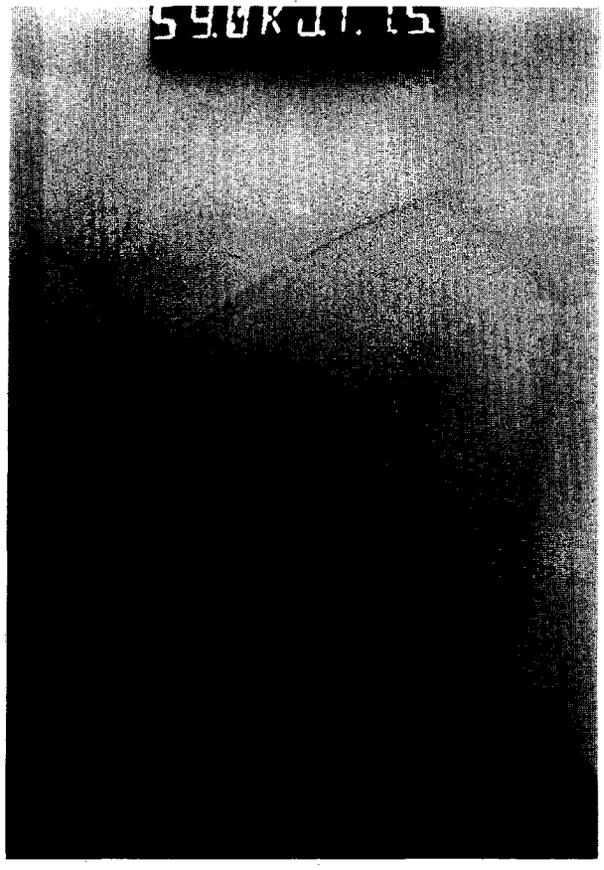

Fig. 11. Transmission electron micrograph of sample 3, for material sintered with C in N_2 at 2100°C, showing triple points. The length of the bar is 420 nm.

Fig. 13. Transmission electron micrograph of sample 4, for material sintered without C in N_2 at 2100°C, showing SiC grains. The length of the bar is 3·1 μm.

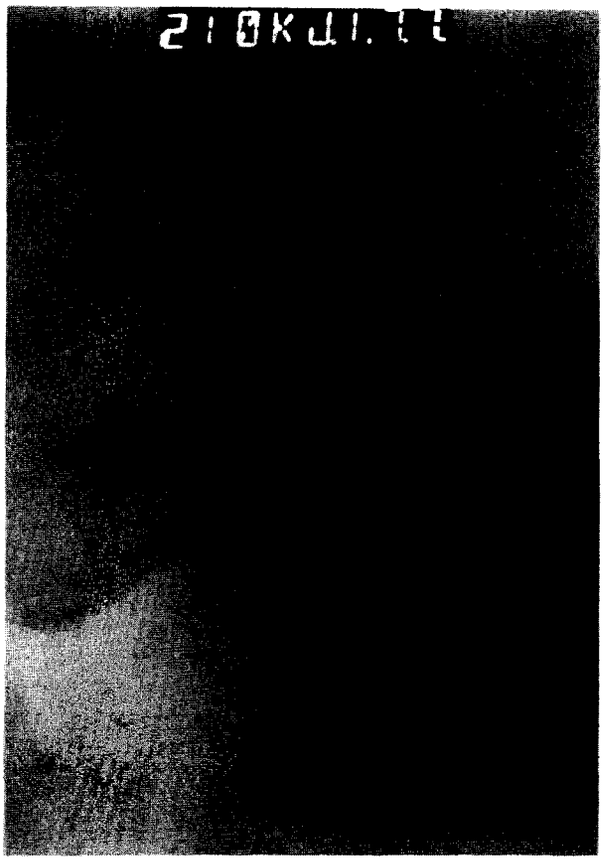

Fig. 12. Transmission electron micrograph of sample 3, for material sintered with C in N_2 at 2100°C, showing an inclusion at the grain boundary. The length of the bar is 120 nm.

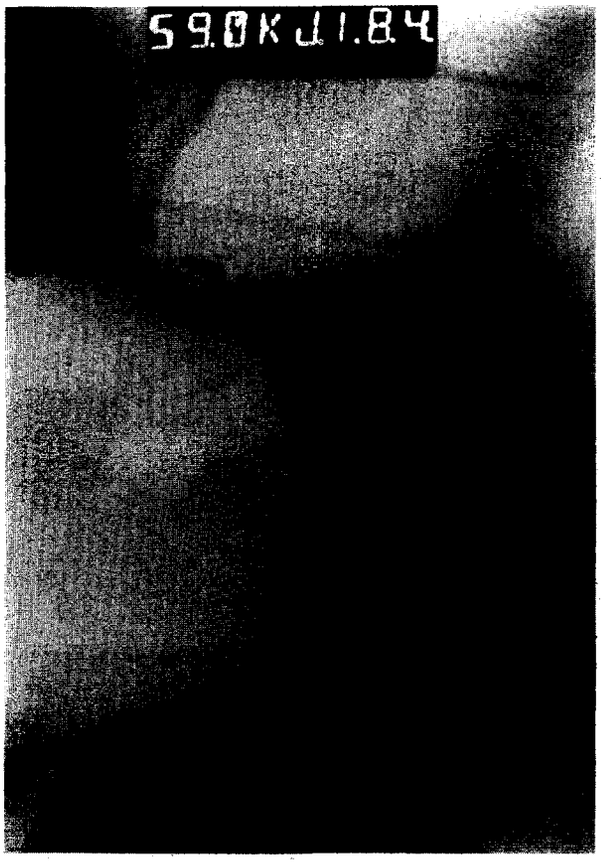

Fig. 14. Transmission electron micrograph of sample 4, for material sintered without C in N_2 at 2100°C, showing triple points. The length of the bar is 420 nm.

phase can partially penetrate the grain boundaries. EDX revealed that the second phase consists of Y–Al–O and Y–Al–O–C. This means that the second phase is free of Si or, more accurately, that the silicon content is lower than the detection limit of 3 wt%. Figure 7 shows a grain boundary in sample 1. No second phase is detected at the grain boundary.

Figure 8 shows the rounded grains of SiC in sample 2. Figure 9 shows a triple point in sample 2. Note the improved wetting of the SiC by the second phase, as indicated by an angle of 40–50°.[14] EDX revealed that the second phase consists of Y–Al–Si–O. The silicon content is between 5 and 10 wt%, which is just above the detection limit. No second phase is detected at the grain boundary.

Figure 10 shows the SiC grains in sample 3. Note that some of the triple points contain a second phase, while other triple points are free from second-phase material. This is shown even better in Fig. 11. EDX showed that the second phase is yttria and Y–Al–O. No second phase is observed at the grain boundary. However, many small inclusions are observed at the grain boundary. EDX revealed that they are yttria and AlN. Figure 12 shows such an inclusion.

Figure 13 shows the SiC grains in sample 4. Except for the grain size, no differences between samples 3 and 4 are observed. Some of the triple points contain a second phase, while other triple points are free from second-phase material, as shown in Fig. 14. EDX showed that the second phase is yttria and Y–Al–O. No second phase is detected at the grain boundary phase. Some small inclusions of yttria and AlN are observed at the grain boundary. XRD performed on sample 2 showed the phases SiC and YAG.

5 Discussion

There is excellent agreement between the theoretical aspects and experimental results. When sintering in Ar at 1900°C, weight loss can be limited by the use of carbon as a sintering additive; very little aluminium vaporizes off. The use of carbon as a sintering additive has no negative effect on sintering rate or the microstructure of the sintered material. It is suggested that the liquid phase is free of silica when carbon is used as a sintering additive. Similar remarks hold for the crystalline phases after cooling of the sintered material. No amorphous phases were found in the material after sintering in Ar at 1900°C with C. Owing to the absence of silica, this is to be expected. Therefore, liquid phase sintering of SiC is more similar to the sintering of AlN to the sintering of Si_3N_4. This is in agreement with the literature.[11]

When sintering in N_2, AlN is formed and will dissolve in the SiC grains during sintering, as known from the phase diagram of SiC–AlN.[7] Upon cooling the AlN leaves the SiC grains and precipitates at the grain boundaries.

By using a SiC powder with a specific surface area of 10 $m^2\ g^{-1}$, mixed with 4 wt% yttria and 6 wt% alumina (sample 2), it is possible to sinter the material in a closed graphite crucible without a powder bed at 1900°C in Ar for 2 h with ~6% weight loss. This weight loss is generally acceptable.

Especially by using carbon as an additive, an interesting SiC material is obtained. The microhardness is 26 GPa, which is similar to sintered SiC prepared with B and C as dopants. The production costs of parts made from LP-SiC should be equal to those made of SiC sintered with B and C.

6 Conclusions

LP-SiC is an excellent material, especially when carbon is used as a sintering additive. Sintering in Ar at 1900°C is recommended. When C is used, the second phase is free of silica, crystalline and less weight loss during sintering is observed. The second phase is present at the triple points and no grain boundary or glassy phases are detected. Excellent high temperature properties are anticipated.

Acknowledgement

A grant from the EU is gratefully acknowledged.

References

1. Omori, M. & Takei, H., *J. Am. Ceram. Soc.*, **65** (1982) C-92.
2. Kostic, E., *Powder Metall Int.*, **20** (1988) 28–9.
3. Trigg, M. B., Australian Patent 00518, 1990.
4. Omori, M. *et al.*, US Patent 4 564 490, 1986.
5. Suzuki, K., *Silicon Carbide Ceramics Vol 2*, eds S. Somiya and Y. Inomata. Elsevier Applied Science, London, 1991, pp. 163–82
6. Trigg, M. B., Australian Patent 00271, 1988.
7. Böcker, W. D. G., European Patent 419271 A2, 1990.
8. Hamminger, R., Krüner, H. & Böcker, W., *J. Hard Mater.*, **3** (1992) 93–107.
9. Mulla, M. A. & Krstic, V. D., *Ceram. Bull.*, **70** (1990) 439–43.
10. Cutler, R. A. & Jackson, T. B., *Ceramic Materials and Components for Engines*, ed. V. J. Tennery. American Ceramic Soc. Inc., Columbus, OH, 1989, pp. 309–18a.
11. Böcker, W. & Hamminger, R., *Interceram*, **40** (1991) 520–5.

12. Private communication with the Carborundum Company in Niagara Falls on Hexoloy SX.
13. Private communication within Lonza-Werke Waldshut on ultra-fine SiC powders.
14. Kingery, W. D., Bowen, H. K. & Uhlmann, D. R., *Introduction to Ceramics*, 2nd edn. J. Wiley and Sons, Inc., New York, 1976.
15. Komp, G., PhD Thesis, University of Technology, Berlin, 1991.
16. Cutler, R. A. *et al.*, US Patent 4 829 027, 1989.